New Late Pleistocene species of *Acharax* from Arctic methane seeps off Svalbard

Jesper Hansen[a]*, Mohamed M. Ezat[b,c,d], Emmelie K. L. Åström[b,e] & Tine L. Rasmussen[b]

[a] Akvaplan-niva AS, Fram Centre – High North Research Centre, NO-9296 Tromsø, Norway.

[b] CAGE - Centre for Arctic Gas Hydrate, Environment and Climate, Department of Geosciences, UiT, The Arctic University of Norway, NO-9037 Tromsø, Norway.

[c] Godwin Laboratory for Palaeoclimate Research, Department of Earth Sciences, University of Cambridge, Cambridge CB2 3EQ, United Kingdom.

[d] Department of Geology, Faculty of Science, Beni-Suef University, Beni-Suef, Egypt.

[e] Department of Arctic and Marine Biology, UiT, The Arctic University of Norway, NO-9037 Tromsø, Norway

Corresponding author, Email: jha@akvaplan.niva.no

We report, for the first time, the solemyid *Acharax svalbardensis* n. sp., from deep-sea methane seep sites on the western Svalbard margin, 79°N. This species is rather small and so far the northernmost representative of its genus. It is identified based on the combination of diagnostic characters: umbo 27–30% valve length from posterior margin; H/L-ratio ~0.35; broadly rounded to truncated anterior margin; 15 moderately developed, flat double-ribs with middle ribs about as strong as posterior ribs. The shells from *Acharax svalbardensis* n. sp. were found in sediment cores from two pockmarks at Vestnesa Ridge at ~1200 m water depth in the Fram Strait off NW Spitsbergen, Svalbard archipelago. Previously, the vesicomyid bivalves *Archivesica arctica* and *Isorropodon nyeggaensis* have been documented from the same pockmarks. Here, we describe the new solemyid species and report its stratigraphic occurrence and co-occurrence with the previously described methane seep-associated vesicomyids. All findings of the vesicomyids and the new solemyid species are restricted to the time interval ~19,000–15,600 cal. years BP, correlating with Heinrich Stadial HS1. This period was characterized by cold surface conditions and extensive ice rafting from sea ice and icebergs in the North Atlantic and Arctic region. Inflow of a warm subsurface current of Atlantic water below the melt water layer led to higher bottom-water temperatures at the Svalbard margin than at present. This increase in bottom-water temperature probably allowed several methane seep-associated bivalve species to settle for a short period of time, namely the vesicomyids *A. arctica* and *I. nyeggaensis* and the new species of the solemyid bivalve genus *Acharax* described here.

Key words: Bivalvia; Chemosymbiotic; *Acharax svalbardensis* n. sp.; Solemyidae; Heinrich Stadial HS1; bottom water temperature.

Introduction

Bivalves are common in chemosynthetic habitats such as methane seeps, and include many chemosymbiotic species within the families and subfamilies Bathymodiolinae, Lucinidae, Solemyidae, Thyasiridae and Vesicomyidae (Taylor & Glover 2010). Arctic methane seeps, located off the archipelago of Svalbard (74˚N - 80˚N), have in recent years been targeted for benthic faunal community studies (Åström *et al.* 2016, 2017a, b; Hansen *et al.* 2017; Sen *et al.* 2018). Geographically, these studied methane seeps span over a large bathymetric range along the western Svalbard margin, where active methane seeps have been documented in the Storfjord Trough at 350–390 m water depth; west of Prins Karls Forland at 350 m water depth; and at Vestnesa Ridge in the Fram Strait at ~1200 m water depth (Fig. 1). Despite the many cold seeps and the widespread sea-bed methane seepage around Svalbard, there are only few records of chemosymbiotically associated bivalves. At Vestnesa, Åström *et al.* (2017a) found, that even though the composition of the molluscan fauna at these methane seeps is markedly different from faunal communities in surrounding non-seep areas, no methane seep-associated chemosymbiotic bivalves were found. Recent investigations however, of marine gravity cores from ~1200 m water depth at Vestnesa Ridge have revealed that the presence of putatively chemosymbiotic molluscs was notable in the past at ~19,000–15,600 cal. years BP (recalibrated herein after Ambrose *et al.* (2015), Hansen *et al.* (2017) and Sztybor & Rasmussen (2017a, b)). These molluscs are the vesicomyid bivalves *Archivesica arctica* and *Isorropodon nyeggaensis* (Ambrose *et al.* 2015; Hansen *et al.* 2017). The period of time correlates to Heinrich Stadial HS1 (~19,000–14,700 cal. years BP e.g., Barker *et al.* 2009), when the bottom water in the Nordic seas and at the Svalbard margin was warmer than at present (e.g. Rasmussen & Thomsen 2004; Rasmussen *et al.* 2007; Ezat *et al.* 2014; Sztybor & Rasmussen 2017a, b) despite it being a climatically cold period in the North Atlantic region (e.g. Bond *et al.* 1993; Dansgaard *et al.* 1993; Hoff *et al.* 2016). Furthermore, shallower

methane seeps along the Prins Karls Forland shelf and Storfjord Through (~350 m water depth) were, at least in the past, inhabited by the seep-associated thyasirid species *Rhacothyas kolgae* and *Thyasira capitanea* (Åström *et al*. 2017b), which are thought to have colonized these areas after the deglaciation of the Barents Sea Ice Sheet (after ~15,000 cal. years BP) (Åström *et al*. 2017b).

Here, we describe one novel fifth methane seep-associated and putatively chemosymbiotic bivalve species from Svalbard. This species, documented from three gravity cores collected at Vestnesa Ridge, belongs to the family Solemyidae and occurs in deposits of HS1-age (Figs 1, 2).

Material and methods

Specimens of *Acharax* have been collected from three cores HH15-1241GC, HH13-203GC, and HH13-211GC. Gravity core HH15-1241GC was sampled at Vestnesa Ridge, eastern Fram Strait, during a cruise with RV Helmer Hanssen (79°00.214´N, 06°55.904´E, 1205 m water depth) 24th of July, 2015 (Rasmussen *et al.* 2015) (Fig. 1). The core was collected from the deepest part in the centre of an active methane seeping pockmark where acoustic reflections from bubble flares were detected with single beam echo sounder. After opening of the core, one of the 10 cm wide core halves was sampled, while the other half was stored as an archive. The stratigraphic occurrences were noted and the shells sampled after visual examination of the core and through sieving of sediment samples.

Gravity cores HH-13-203GC (79°00.144´N, 06°55.683´E, 1210 m water depth) and HH-13-211GC (79°01.867´N, 06°49.851´E, 1202 m water depth) were taken the 13th and 14th of October 2013 respectively, from two pockmarks at Vestnesa Ridge during a scientific cruise

with RV Helmer Hanssen (Mienert 2013) (Fig. 1). These two cores were previously investigated by Ambrose *et al.* (2015). Both cores have a diameter of 10 cm. Core HH-13-203GC was collected at an active gas flare site in the same pockmark as cores JM10-335GC (Sztybor & Rasmussen 2017a) and HH15-1241GC (this study). Core HH-13-211GC was collected at a nearby pockmark (Fig. 1), for which no acoustic flares were detected during sampling in 2013. However, flares have previously been documented by Bünz *et al.* (2012) and again in 2018 by Rasmussen *et al*. (2018). Solemyid shell fragments from both cores were sorted out from sieved sediment samples (1 mm mesh-size) (for details see Ambrose *et al.* 2015).

For core HH15-1241GC, radiocarbon dates were performed on four samples of the planktonic foraminiferal species *Neogloboquadrina pachyderma* (Table 1). All dates and previously published ^{14}C dates have been recalibrated using the Calib7.04 and the Marine13 program and the reservoir age correction of 405 years inherent in the program (Stuiver & Reimar 1993; Reimar *et al.* 2013). This age is close to modern reservoir age of the surface ocean in the open Nordic seas of 400 years with a ΔR of 7±11 years (Mangerud *et al.* 2006).

All shells showed damage from sedimentary compaction and core sampling. It is uncertain how complete the specimens recovered by sieving were before sampling. Shell fragments of little taxonomic value were not used. The holotype is broken in several pieces, but is otherwise intact except for a post-mortem loss of a thin slice of the valve edge at the anteroventral margin of the right valve (Figs 3, 4).

Results

Stratigraphy and correlation of cores

Radiocarbon dating of vesicomyids from the shell interval in core HH-13-203GC published by Ambrose *et al.* (2015) gave a ^{14}C age of 14,230±50 years BP, which by recalibration resulted in an age of 16,735±130 cal. years BP (Fig. 2). Two published recalibrated ages from vesicomyid shells from core HH13-211 gave ages of 17,585±90 and 17,735±95 cal. years BP. These dates are all typical for Heinrich Stadial HS1. Dates performed on *N. pachyderma* from the same two cores indicated too old ages, probably due to contamination from authigenic carbonate overgrowth, which is a general problem at seep sites (Uchida *et al*. 2008; Ambrose *et al.* 2015). Therefore, we use the characteristic lithological features stacked from 11 slope records from the western Svalbard margin published by Jessen *et al.* (2010) to generate a general stratigraphy of the cores (Fig. 2). All ^{14}C ages from the stacked record of Jessen *et al.* (2010) have been recalibrated similarly to the dates from the three cores of this study (see methods above) (Fig. 2). Furthermore, we recalibrated ages from the previously published record JM10-335GC, which was correlated closely to the stack record of Jessen *et al.* (2010) (Sztybor & Rasmussen 2017a) (same position as HH13-203GC) (Figs 1, 2). Three lithological units (a mass flow/ice-rafted debris (IRD) layer dating ~24,000 cal. years BP, a laminated deposit from the Bølling interstadial dating ~15,100–14,600 cal. years BP, and a Holocene diatom layer dated to ~10,000 cal. years BP) occur in core HH15-1241GC, while cores HH13-203GC and HH13-211GC do not reach into the mass flow/IRD layer (Fig. 2). From the correlation based on lithology supported with ^{14}C ages it is clear that the *Acharax* shells occur in sediments dating between 19,000 and 15,600 cal. years BP, correlating to Heinrich Stadial HS1 (Fig. 2). This time-interval is similar as for the previously described vesicomyid bivalves from Vestnesa Ridge (Ambrose *et al.* 2015; Hansen *et al.* 2017; Sztybor & Rasmussen 2017a, b). By this correlation to known lithology it is also clear that the three upper radiocarbon ages, which were performed on *N. pachyderma* from core HH15-1241GC, are too old (Fig. 2; Table 1), similar to the ages reported by Ambrose *et al.* (2015).

Reposition of type specimens

The type specimens are deposited in the geological collections (TSGF-numbers) at the Tromsø University Museum, NO-9037 Tromsø, Norway.

Systematic descriptions

Class **Bivalvia** Linnaeus, 1758

Order **Solemyoida** Dall, 1889

Family **Solemyidae** Gray, 1840

Genus ***Acharax*** Dall, 1908a

Type species. *Solemya johnsoni* Dall, 1891

Diagnosis. Solemyidae with ligament external as a high arched band. Full diagnosis is provided by Kamenev (2009)

Acharax svalbardensis n. sp.

(Figs 3–5)

Diagnosis. Small to medium-sized *Acharax* reaching a length of at least 70 mm. Elongate, rounded subrectangular outline. Umbo 27–30% valve length from posterior margin. Subparallel dorsal and ventral margins. H/L-ratio of valves ~0.35. Broadly rounded to truncated anterior margin. Sculpture of 15 moderately developed, flat double-ribs with middle ribs about as strong as posterior ribs.

Derivation of name. '*svalbardensis*' refers to Svalbard archipelago from where it has been recorded.

ZooBank registration. urn: ---- [to be provided in case of acceptance of manuscript]

Type material. Holotype, crushed but entire shell, TSGF 18407, core HH15-1241 GC, core depth 248–250 cm; paratype 1, fragment of right valve, TSGF 18408, core HH-13-203 GC, core depth 242–250 cm; paratype 2, fragment of right valve, TSGF 18409, core HH-13-211 GC, core depth 421–426 cm; paratype 3, broken specimen, TSGF 18410, core HH15-1241 GC, core depth 219–221 cm; paratype 4, broken left valve, TSGF 18411, core HH-13-211 GC, core depth 421–426 cm; paratype 5, fragment of left valve, TSGF 18412, core HH-13-211 GC, core depth 417–421 cm; paratype 6, fragment of left valve, TSGF 18413, core HH-13-211 GC, core depth 405–408 cm; paratype 7, fragment of left valve, TSGF 18414, core HH-13-211 GC, core depth 421–426 cm; paratype 8, broken right valve, TSGF 18415, core HH-13-211 GC, core depth 421–426 cm; paratype 9, broken right valve, TSGF 18416, core HH-13-203 GC, core depth 243–246 cm; paratype 10, fragment of left valve, TSGF 18417, core HH-13-211 GC, core depth 421–426 cm.

Type locality. Core HH15-1241GC (79°00.214´N, 06°55.904´E, 1205 m water depth), Vestnesa Ridge, Fram Strait, NW Spitsbergen, Svalbard archipelago.

Description. Shell rather small to medium sized, with holotype ~36 mm long and 12.5 mm high (H/L-ratio = 0.35 (~0.32–0.35 on growth lines of holotype and paratypes, taking into account that the umbonal valve margin is partly resorbed during shell growth)), and slightly

deeper at 1/4 valve length from anterior margin of valve than at umbo. Size estimates of fragments indicate a size range from 20 to 70 mm in length, with the majority between 30 and 50 mm. Broad and flattened umbo located at ~27–30% (measured on growth lines or valve outline of seven valves) valve length from posterior margin. Shell equivalve with moderately robust valves. Outline (based on outlines and a study of growth lines of all specimens) elongate, rounded subrectangular with length about three times of height. Valves somewhat compressed. Dorsal and ventral margins subparallel. Anterior margin broadly rounded to truncated perpendicular to dorsal and ventral margins, becoming more truncated with size. Posteroventral margin narrowly rounded, with gently convex to nearly straight posterodorsal margin defining an angle of ~155°–160° on the dorsal margin at umbo. Umbo with indistinct beak. Periostracum yellowish brown, darkening to blackish brown at margins. Sculpture of 15 very flat, widely spaced radial double-ribs, with ten in front and five posterior. The ribs are strongest developed in the anterior-most part of the shell. A rather narrow, smooth median area equalling the combined width of one rib and two interspaces separates posterior part from anterior. Posterior ribs in several specimens darker than the interspaces. Posterior most part of shell without ribs.

Opisthodetic ligament external and supported by a thickened shell margin. Hinge teeth absent, but nymph rather prominent and extending over half the distance from umbo to posterior end. Anterior adductor scar large and subtriangular with evenly rounded anteroventral margin and nearly straight dorsal and posterior margins. Its length ~15–18% valve length based on holotype and estimates on paratypes. Anterior pedal retractor scar deeply impressed, elongate subtriangular and bordering adductor scar posterodorsally. Posterior adductor scar rather deeply impressed subrectangular and about two-third the size of the anterior adductor scar or ~10–13% length of valve. The size of muscle scars compared to shell size seems not to change with growth. External sculpture weakly impressed on interior

of valves, especially close to valve margins. Pallial line is simple, running close to ventral valve margin, and connecting medioventrally to adductor scars.

Distribution. The specimens are from a methane seep environment at 1202–1210 m water depth on the Vestnesa Ridge in the Fram Strait, NW Spitsbergen, Svalbard. All specimens are dated to ~19,000–15,600 cal. years BP. At that time the global mean sea level was ~110–80 m lower than at present (Fairbanks 1989).

Comparisons. Due to the fragmented state of the specimens, it is problematic to get exact measurements of maximum size. However, assuming a relatively stable outline of the shells during growth as supported by the growth-lines, it is possible to get a coarse estimate of the size range of the available specimens. The 11 specimens show a size range from 20 to 70 mm in length, with the majority (eight specimens) between 30 and 50 mm in length. Even though the specimens have rather fragile shells, at least two individuals had conjoined valves. It is likely that these individuals were found in their original habitat and have not been subject to transport or size sorting. Furthermore, since the shells of the new solemyid species originate from three cores penetrating different parts of the methane seeping pockmarks, as well as representing an interval of several thousand years, we assume that the material represents the normal size range of the species.

Presently there are 9 extant species recognized within the genus *Acharax*, as well as about 23 fossil species among which most are from the Pacific region. Comparison has been made with all recognized species, but here we include only the Neogene species. All species differed in more than just their size. The comparisons with the extant species assigned to the genus are partly based on the updated information provided by Huber (2010). Some of the main characteristic differences are presented in Table 2.

Acharax svalbardensis n. sp. is close to the extant NE Atlantic species *A. gadirae* Oliver, Rodrigues & Cunha, 2011 found and described from the Gulf of Cadiz off Portugal, Spain and Morocco. *A. gadirae* reach a size of 67 mm length, but it differs by a consistently higher H/L-ratio of 0.37 on four mature specimens and 0.37–0.48 on five immature specimens ~10 mm long (including one illustrated by Rueda *et al*. (2012)); more pointed anterodorsal corner; generally more oblique anterior margin with less defined transition to ventral side; and by the ribs in the middle part of the shell being consistently poorly developed making the smooth median area seem very broad, whereas on the new species *A. svalbardensis* they are consistently as well developed as in the posterior part of the shell (Figs 3–5).

Acharax alinae Métivier & Cosel, 1993 from near the Fiji Islands in the South Pacific is up to 106 mm long and is distinguished by an H/L-ratio of 0.43; umbo 1/3 valve length from posterior valve margin; 16–17 rather strong ribs, and anterior margin similar to that of *A. gadirae*.

Acharax bartschii (Dall, 1908b) from the Philippines is up to 191 mm long; with the umbo at ~36% valve length from the posterior valve margin; and a very wide median area without radiate ornamentation between the anterior and the posterior ribs.

Acharax burica Olsson, 1942 from the Pliocene of Panama is estimated to have been ~115 mm long and differs by an H/L-ratio of ~0.41; by the broad and flat-topped posterior ribs, and radiate striation in the broad median area between the anterior and the posterior ribs.

Acharax caribbaea (Vokes, 1970) from Louisiana is up to 78.3 mm long. It can be distinguished on its higher H/L-ratio of ~0.36–0.41; only four to five distinct, low anterior ribs with many second and third order ribs on top and in between; very poorly developed ribs in the median part of the shell, and three distinct ribs in the posterior part.

Acharax clarificata Dell, 1995 from New Zealand is up to 88 mm long and differs by an H/L-ratio of 0.36–0.39; dark reddish brown to blackish periostracum, and ribs weakly developed in the middle part (see Walton 2015).

Acharax doderleini (Mayer, 1861) from the Miocene and Pliocene of Italy is up to 101 mm long and has, according to illustrations by Taviani *et al*. (2011), an H/L-ratio of 0.28–0.33 (mostly 0.30 or lower); umbo located at ~23–27% valve length from posterior margin; and has very weak median ribs similar to *A. gadirae*.

Acharax gigas (Kanno, 1960) from the Miocene of Japan is up to 264 mm long and has very poorly developed ribs in the middle part, while the ribs in the posterior and anterior part are moderately developed.

Acharax grandis (Verrill & Bush, 1898) from the Northwest Atlantic off Virginia is up to at least 70 mm long, with an H/L-ratio of ~0.36, but has the umbo much closer to the mid-line of the valves, and a strongly developed nymph supporting the ligament.

Acharax johnsoni (Dall, 1891), which presently is thought to include specimens from the Lower Miocene to Recent of the Pacific region (see Sasaki *et al*. 2005), is up to 150 mm long and is morphologically very variable. A molecular study by Neulinger *et al.* (2006) has shown that it is a species complex of at least two extant species, probably explaining some of its large morphological variability. The species complex encompasses many features resembling those of the specimens from Svalbard externally as well as internally. However, the complex seems to differ in that the median one to three ribs nearly always are markedly weaker than the rest. The original specimen of Dall (1891) is 115 mm long and with an H/L-ratio of 0.42. We believe more differences will be revealed when the morphologic characters of *Acharax johnsoni* sensu stricto have been reanalysed. Geographically *A. johnsoni* and *A. svalbardensis* are separated by the American continent and major oceanic current systems.

Acharax muroensis (Natori, 1964) from the Upper Oligocene or lowermost Miocene of Japan is based on a poorly preserved and broken valve, but is at least 22 mm long. According to description and illustration, it differs by having strongest ribs around midvalve length, while posterior and anterior ribs are weak. It also differs in that the posterodorsal margin of the shell is much more excavated. By tracing growth lines, the umbo is located at ~1/5 valve length from posterior margin and the anterior outline resembles that of *A. gadirae*.

Acharax patagonica (Smith, 1885) from the SE Pacific off Chile is up to 62 mm long and can be distinguished on its elongate suboval outline and weaker developed or absent posterior and middle ribs.

Acharax prashadi (Vokes, 1955) (including *A. eremita* in Kuznetsov & Shileyko 1984) from the West Indian Ocean and Gulf of Aden is up to 100 mm long. It has about the same H/L-ratio of 0.33–0.36, but is distinguished by the poorly developed ribs, especially in the entire middle part of the valves; the dark colour of all ribs; and by that the umbo is slightly closer to the posterior margin, at ~22–27% valve length.

Acharax subquadrata (Foresti, 1879) from the Miocene of Italy is at least 86 mm long, and differs by an H/L-ratio of ~0.38–0.41, umbo at 24% valve length from posterior margin; and a very angular outline (see Taviani *et al*. 2011).

Acharax subventricosta Krishtofovich in Gladenkov *et al.* (1984) from the Neogene of Western Kamchatka is ~50 mm long and is distinguished by having a broader rounded posterior margin; a greater H/L-ratio of ~0.4; and umbo located at ~1/3 valve length from posterior margin.

Acharax ventricosa (Conrad, 1849) from the Miocene and Pliocene of Western USA is more than 100 mm long and has an H/L-ratio of ~0.35–0.44, and an anterior margin very similar to that of *A. gadirae* (see Moore 1963).

Acharax yessoensis (Kanehara, 1937) from the Miocene of Japan is 84 mm long and differs by its H/L-ratio of 0.31; valve anterodorsally pointed, and anterior margin goes almost continuously into ventral margin.

Acharax yokosukensis Kanie & Kuramochi, 1995 from the Miocene of Japan is exceeding 295 mm in length, has an umbo situated between 39–48% valve length from posterior valve margin; an H/L ratio of 0.39–0.44 and has only 14 ribs (see Amano & Ando 2011).

Discussion

Spatial and temporal distribution of *Acharax svalbardensis* n. sp.

To present date, there are no records of live specimens of *Acharax svalbardensis* n. sp., nor any other living methane seep-associated chemosymbiotic bivalve species in the Svalbard-Barents Sea region, as well as in the Arctic Ocean and the Nordic seas, except thyasirids (Rachor 1997; Gebruk *et al.* 2003; Krylova *et al*. 2011; Decker & Olu 2012; Åström *et al.* 2016; Åström *et al.* 2017a, b; Hansen *et al*. 2017; Sen *et al.* 2018). Therefore it appears that the species is absent from the area in Modern times and possibly extinct. *Acharax svalbardensis* n. sp. seems restricted to Heinrich Stadial HS1 ~19,000–15,600 cal. years BP, when cold surface conditions prevailed in the North Atlantic and Arctic region (Bond *et al.* 1993; Fronval *et al.* 1995; Cronin *et al.* 2012; Ezat *et al*. 2016; Hoff *et al.* 2016). This is the same pattern that was observed by Hansen *et al.* (2017) for the co-occurring methane seep-associated vesicomyid bivalves *Archivesica arctica* and *Isorropodon nyeggaensis* at Vestnesa Ridge. Hansen *et al.* (2017) speculated that the presence of the vesicomyids in the area, including similar old specimens at the Gakkel Ridge in the Arctic Ocean, was made possible by the short-lived increase in bottom-water temperature due to a subsurface current of

northward advection of Atlantic water below the cold meltwater layer, which led to >2°C warmer bottom-water temperatures than in Modern times (Rasmussen *et al.* 2007, 2014; Ezat *et al.* 2014, 2016; Sztybor & Rasmussen 2017a, b). Presently, at Vestnesa Ridge, where the new species *A. svalbardensis* n. sp. is found, bottom water temperatures are ~-0.9° to -0.8°C (Aagaard *et al*. 1985; Åström *et al*. 2017a). If bottom water temperature was the restricting factor of the distribution of *A. svalbardensis* n. sp. similarly as for the vesicomyids, live communities could be found at deep-sea methane seeps at lower latitudes, if still extant.

Climatic controls on the genus *Acharax* through time

In his treatise on fossil and extant solemyids, Vokes (1955) found evidence that the bathymetric distribution of the genus *Acharax* was controlled by temperature, with the deepest occurrences of the individual species found near the Equator. There have been an increasing number of reported sites with living *Acharax* spp., which has made the general picture of their distribution more complex. Nonetheless, it seems that there is a trend of generally shallower both minimum and maximum depths farthest away from the Equator, both at species level and within the widespread *A. johnsoni* species complex (see e.g. Vokes 1955 and Kamenev 2009). This distribution could indicate that *Acharax* has a preferred temperature range. Similarly, Taylor & Glover (2010) noted that the geographical ranges of extant species of the family Solemyidae are limited to tropical to temperate latitudes. Live *Acharax* specimens have not been reported from farther south than off South America at 53°S or been observed north of 60°N in the northern Pacific (Huber 2015). The geographical distribution of fossil *Acharax* species shows that the northernmost species previously reported is the Eocene *Acharax tigilensis* (Krishtofovich in Devjatilova & Volobueva 1981) from the Siberian Anadyr River at ~65°N, while the southernmost report is of the Oligocene *Acharax belenensis* Olsson, 1931 in Peru, at ~5°S. More recently, Amano & Ando (2011) observed that the largest species

within both the chemosymbiotic bivalve taxa *Acharax* and Lucinidae occurs in geological periods or regions with warmer climates, and suggested that size is more dependent on temperature and food supply than water depth. However, while we agree with this suggestion by reviewing existing literature, the size of *Acharax*-species is in geological perspective evidently also increasing as a result of evolution. Despite several warmer periods before the Miocene (e.g., Zachos *et al.* 2001) there are hitherto no reports of specimens exceeding 90 mm length prior to the Miocene, while there are many reports of this size class from the Miocene and after. All these observations on temperature dependence corresponds well with that *Acharax svalbardensis* n. sp. is a relatively small member of the genus and also supports the hypothesis that temperature is an important limiting factor for the distribution of the species.

Faunal characteristics of deep-sea Arctic methane seeps

Present day Modern macrofaunal communities from deep-sea methane seeps at high northern latitudes are substantially different from those of comparable non-seep habitats and dominated by chemosymbiotic worms (Siboglinidae) (e.g. Gebruk *et al*. 2003; Vanreusel *et al.* 2009; Krylova *et al*. 2011; Åström *et al*. 2017a). However, most species from these communities, such as the abundant *Thyasira* aff. *dunbari* (an undescribed bivalve species commonly assigned to the North American *T. dunbari*), are not restricted to the seep habitats (Gebruk *et al*. 2003; Åström *et al*. 2017a). In a similar manner, the still poorly investigated Antarctic region seems to lack well-developed seep-endemic chemosymbiotic communities even though vesicomyid shell layers show such existed in the past (see German *et al*. 2011). In contrast, lower latitude seep and vent systems from >200 m water depth sustain well-developed chemosymbiotic communities, characteristically inhabited by vent and seep molluscs such as Vesicomyidae, Lucinidae, Solemyidae and small gastropods (e.g. *Provanna*) (Sahling *et al.*

2003; Sweetman *et al*. 2013; Hryniewicz *et al*. 2015a; Levin *et al.* 2016). The Modern Molluscan macrofauna at the Vestnesa Ridge methane seeps is a typical Arctic deep-water methane seep fauna comprised of opportunistic non-seep species (Gebruk *et al*. 2003; Åström *et al*. 2017a).

Two main hypotheses have been proposed as explanations for the lack of the lower latitude deep-water seep-, and vent endemic mollusc faunas in the Arctic region (Pedersen *et al*. 2010; Sweetman *et al*. 2013; Hansen *et al*. 2017); 1) the Greenland-Scotland Ridge forms a migration barrier; and/or 2) the sub-zero (°C) bottom-water temperatures in the Arctic region are too cold for characteristic seep-, and vent- mollusc faunas to compete with the conventional non-seep fauna in the region. Since both vesicomyids and solemyids inhabited Vestnesa Ridge during HS1, and that vesicomyids also occur in deposits of similar age at the Gakkel Ridge in the Arctic Ocean, as well as in deposits at the Nyegga methane seep in the Norwegian Sea (Rachor 1997; Krylova *et al*. 2011; Hansen *et al*. 2017; herein), we can rule out the first hypothesis. This leaves restriction by temperature as the most likely hypothesis for their past presence and current apparent absence in the region. So far we have noted, all documented live occurrences of typical chemosymbiotic deep-sea seep molluscs are from places with bottom water temperatures of >1°C at least during summer, even in the East Russian Sea of Okhotsk (e.g. Tomczak & Godfrey 1994; Sahling *et al*. 2003; Kamenev 2009, 2017). Seep-associated bivalves have been present at Svalbard methane seeps as far back as the Late Jurassic and Early Cretaceous (Hryniewicz *et al*. 2014, 2015b). However, these communities evolved during very different and much warmer conditions and at a more southern palaeogeographic position compared to today's Arctic environment (Zakharov *et al*. 2002). According to Plaza-Faverola *et al.* (2015) methane seepage at Vestnesa Ridge has been active for the past 2.7 million years, in principle leaving enough time for Arctic chemosymbiotic seep communities to evolve. The fact that no such communities are observed

today leads us to infer that seepage may have been insufficient or dormant over periods of time.

Bathymetric gradients of seep faunas off Svalbard compared to the Sea of Okhotsk

Along the Svalbard-Barents Sea margin several present-day methane seeps emits methane at water depths between 80–400 m, which is near the predicted upper depth limit of the gas hydrate stability-zone (Westbrook *et al.* 2009; Sahling *et al.* 2014; Portnov *et al.* 2016; Mau *et al.* 2017). The benthic community-composition at these active seeps compared to the deeper Vestnesa Ridge shows a substantial bathymetric gradient. At seep-sites at the Svalbard deep shelf/upper slope, the faunas are mainly dominated by chemosymbiotic frenulates (Siboglinidae) and the small thyasirid bivalve *Mendicula* cf. *pygmaea* (Åström *et al*. 2016). Empty shells reveal that in the past these seep-sites also hosted the seep-associated larger thyasirids *Thyasira capitanea* and *Rhacothyas kolgae* described by Åström *et al*. (2017b). In comparison, the most dominant organisms at the active deep-sea seeps at Vestnesa Ridge are the crustacean Tanaidacea, Siboglinidae, Oligochaeta and *Thyasira* aff. *dunbari* (Gebruk *et al*. 2003; Åström *et al*. 2017a). In the past, Vestnesa Ridge furthermore hosted colonies of vesicomyids and solemyids (Hansen *et al*. 2017; this study).

Sahling *et al*. (2003) investigated seep-community composition along a bathymetric gradient in the Sea of Okhotsk. They found that seeps at the outer shelf did not host any obvious seep-associated molluscs, however, at the upper slope seeps (370–380 m water depth) empty shells of the seep-associated large thyasirid *Conchocele bisecta* as well as from *Acharax* were observed together with live siboglinids *Siboglinum plumosum*. The intermediate slope seeps (675 m water depth) hosted shell beds of *Conchocele bisecta* and vesicomyid bivalves, where also a few live *C. bisecta* were recorded. At the deep-sea seeps (1450–1600 m water depth), live vesicomyids together with siboglinids were found.

Despite many differences in faunal composition at species and genus level between the two regions, the Sea of Okhotsk and the Svalbard margin, there are striking similarities at higher taxonomic levels. In both regions, there is a bathymetric shift in faunal composition from: 1) the shelf seeps (<250 m) with no documented chemosymbiotic metazoans, though microbial patches are present; 2) upper slope seeps (250–450 m) with faunal communities where siboglinids and at least empty shells of large seep-associated thyasirids occur; 3) the deep-water seeps (1200–1600 m) where siboglinid-vesicomyid communities are noticeable (at present day in the Sea of Okhotsk and in the past, also at Vestnesa Ridge).

Since Sahling *et al*. (2003) found shells of vesicomyids and *Acharax* on the slope, where bottom water temperature can oscillate between -1.7° and 2°C, they excluded temperature as the reason for the absence of vesicomyids from shallower waters in the Sea of Okhotsk. Instead they suggested low oxygen levels, fine-grained sediments and low abundance of predators as likely factors controlling the distribution. It is likely that such factors also have influenced the distribution of the observed chemosymbiotic seep species around Svalbard (Pedersen *et al.* 2010; Schander *et al.* 2010; Sweetman *et al.* 2013; Åström *et al.* 2016; 2017a, 2017b; Sen *et al.* 2018). However, as discussed above, the oceanographic changes and bottom-water temperature increase during HS1 most likely played a major role for the establishment and duration of the seep-associated mollusc faunas at Vestnesa Ridge and at Gakkel Ridge in the Arctic Ocean. The fact that only few chemosymbiotic taxa are documented at methane seeps in the Arctic today despite their presence in the past indicates that both bottom water masses and temperature might be important restrictions on the distribution of such biota (Åström *et al*. 2016; 2017a; Decker & Olu 2012; Paull *et al*. 2015, Hansen *et al*. 2017; Savvichev *et al*. 2018).

Summary and conclusions

We documented a novel Arctic bivalve, *Acharax svalbardensis* n. sp., present in sediment cores from active methane seeping pockmarks at Vestnesa Ridge off Svalbard, 79˚N. The new species, *Acharax svalbardensis* n. sp., co-occurred with recently described vesicomyids, dated to ~19,000–15,600 cal. years BP. This period of time corresponds to the Heinrich Stadial HS1, where surface water conditions were colder and bottom water conditions warmer (up to 2˚C warmer) than today. We suggests that the presence of the new species and its restricted stratigraphic distribution is linked to the warmer bottom water conditions in the North Atlantic and Arctic region during HS1.

Acknowledgements

J.H would like to give a special thanks to his wife Ulrike Hoff, who passed away December 2017, for support, help with literature and work on the figures. It was planned that she should be part on the manuscript, but her strength failed her too early. MM.E is funded by the Research Council of Norway and the Co-funding of Regional, National, and International Programmes (COFUND) – Marie Sklodowska-Curie Actions under the EU Seventh Framework Programme (FP7), project number 274429. This research is also funded by the Research Council of Norway through its Centres of Excellence funding scheme, project number 223259. EKL.Å is funded by a post-doctoral scholarship through VISTA – a research program in collaboration between The Norwegian Academy of Science and Letters, and Equinor. Thanks to the captain and crew on board RV Helmer Hanssen for taking the gravity cores and to S. Vadakkepuliyambatta for help with Figure 1A. We thank Krzysztof

Hryniewicz and two anonymous reviewers for comments that greatly improved the final manuscript.

References

Aagaard, K., Swift, J. H. & **Carmack, E. C.** 1985. Thermohaline circulation in the Arctic Mediterranean Seas. *Journal of Geophysical Research*, **90**, 4833–4846.

Amano, K. & **Ando, H.** 2011. Giant fossil *Acharax* (Bivalvia: Solemyidae) from the Miocene of Japan. *The Nautilus*, **125**, 207–212.

Ambrose, W. G. Jr., Panieri, G., Schneider, A., Plaza-Faverola, A., Carroll, M. L., Åström, E. K. L., Locke, W. L. V. & **Carroll, J.** 2015. Bivalve shell horizons in seafloor pockmarks of the last glacial-interglacial transition: a thousand years of methane emissions in the Arctic Ocean. *Geochemistry, geophysics, geosystems*, **16**, 4108–4129.

Åström, E. K. L., Carroll, M. L., Ambrose, W. G. & **Carroll, J.** 2016. Arctic cold seeps in marine methane hydrate environments: Impacts on shelf macrobenthic community structure offshore Svalbard. *Marine Ecology Progress Series*, **552**, 1–18.

Åström, E. K. L., Carroll, M. L., Ambrose, W. G. Jr., Sen, A., Silyakova, A. & **Carroll, J.** 2017a. Methane cold seeps as biological oases in the high-Arctic deep sea. *Limnology and Oceanography,* **63**, S209–S231.

Åström, E. K. L., Oliver, P. G. & **Carroll, M. L.** 2017b. A new genus and two new species of Thyasiridae associated with methane seeps off Svalbard, Arctic Ocean. *Marine Biology Research*, **13**, 402–416.

Barker, S., Diz, P., Vautravers, M. J., Pike, J., Knorr, G., Hall, I. R., & Broecker, W. S. 2009. Interhemispheric Atlantic seesaw response during the last deglaciation. *Nature*, **457**, 1097–1102.

Bond, G., Broecker, W. S., Johnsen, S. J., McManus, J., Labeyrie, L., Jouzel, J. & Bonani, G. 1993. Correlations between climate records from North Atlantic sediments and Greenland ice. *Nature*, **365**, 143–147.

Bünz, S., Polyanov, S., Vadakkepuliyambatta, S., Consolaro, C. & Mienert, J. 2012. Active gas venting through hydrate-bearing sediments on the Vestnesa Ridge, offshore W-Svalbard. *Marine Geology*, **332–334**, 189–197.

Conrad, T. A. 1849. Fossils from Northwestern America. In: J.D. Dana, The United States Exploring Expedition 1838–1842, under Charles Wilkes. *Geology*, **10**, app. p. 723–72, atlas, pl. 17–21, figs 7, 8.

Cronin, T. M., Dwyer, G. S., Framer, J., Bauch, H. A., Spielhagen, R. F., Jacobsson, M., Nilsson, J., Briggs JR, W. M. & Stepanova, A. 2012. Deep Arctic Ocean warming during the last glacial cycle. *Nature Geoscience*, **5**, 631–634.

Dall, W. H. 1889. On the hinge of pelecypods and its development, with an attempt toward a better subdivision of the group. *American Journal of Science*, **38**, 445–462.

Dall, W. H. 1891. On some new or interesting West American shells obtained from the dredgings of the U.S. Fish Commission steamer 'Albatross' in 1888, and from other sources. *Proceedings of the United States National Museum*, **14**, 173–191.

Dall, W. H. 1908a. A revision of the Solenomyacidae. *The Nautilus*, **22**, 1–2.

Dall, W.H. 1908b. A gigantic Solemya and a new Vesicomya. *The Nautilus*, **22**, 61–63.

Dansgaard, W., Johnsen, S. J., Clausen, H. B., Dahl-Jensen, D., Gundestrup, N. S., Hammer, C. U., Hvidberg, C. S., Steffensen, J. P., Sveinbjörnsdottir, A. E., Jouzel, J.

& Bond, G. 1993. Evidence for general instability of past climate from a 250-kyr ice-core record. *Nature*, **364**, 218–220.

Decker, C. & **Olu, K**. 2012. Habitat heterogeneity influences cold-seep macrofaunal communities within and among seeps along the Norwegian margin – Part 2: contribution of chemosynthesis and nutritional patterns. *Marine Ecology*, **33**, 231–245.

Dell, R.K. 1995. New species and records of deep-water Mollusca from off New Zealand. Tuhinga. *Records of the Museum of New Zealand Te Papa Tongarewa*, **2**, 1–26.

Devjatilova, A. D. & **Volobueva, B. I.** 1981. *Atlas of the Neogene and Paleogene faunas in the North-East USSR*. Nedra Publishing House, Moscow, 219 pp. [in Russian]

Ezat, M. M., Rasmussen, T. L. & **Groeneveld, J.** 2014. Persistent intermediate water warming during cold stadials in the southeastern Nordic seas during the past 65 k.y. *Geology*, **42**, 663–666.

Ezat, M. M., Rasmussen, T. L. & **Groeneveld, J.** 2016. Reconstruction of hydrographic changes in the southern Norwegian Sea during the past 135 kyr and the impact of different foraminiferal Mg/Ca cleaning protocols. *Geochemistry, Geophysics, Geosystems*, **17**, 3420–3436.

Fairbanks, R. G. 1989. A 17,000-years glacio-eustatic sea level record: influence of glacial melting rates on the Younger Dryas event and deep-ocean circulation. *Nature*, **342**, 637–749.

Foresti, L. 1879. Contribuzioni alla Conchiologia fossile italiana. *Memorie della Accademia delle Scienze dell'Istituto di Bologna*, **3**, 111–129.

Fronval, T., Jansen, E., Bloemendal, J. & **Johnsen, S. J.** 1995. Oceanic evidence for coherent fluctuations in Fennoscandian and Laurentide ice sheets on millennium timescales. *Nature*, **374**, 443–446.

Gebruk, A. V., Krylova, E. M., Lein, A. Y., Vinogradov, G. M., Anderson, E., Pimenov, N. V., Cherkashev, G. A. & Crane. K. 2003. Methane seep community of the Håkon Mosby mud volcano (the Norwegian Sea): composition and trophic aspects. *Sarsia*, **88**, 394–403.

German, C. R., Ramirez-Llodra, E., Baker, M. C., Tyler, P. A. & ChEss Scientific Steering Committee 2011. Deep-water chemosynthetic ecosystem research during the Census of Marine Life Decade and Beyond: A proposed Deep-Ocean Road Map. *PLoS ONE*, **6**, e23259.

Gladenkov, Y. B., Gladikova, V. M., Kafanov, A. I., Konova, L. N., Krishtofovich, L. V., Sinelnikova, V. N. & Popov, S. V. 1984. Marine molluscs. *Trudy Geologicheskogo Instituta Akademii Nauk SSSR*, **385**, 152–251, pls. 27–65. [in Russian with English title]

Gray, J. E. 1840. *Synopsis of the contents of the British Museum, 42nd edition*. C. Woodfall & Son, London, 89 pp.

Hansen, J., Hoff, U., Sztybor, K. & Rasmussen, T. L. 2017. Taxonomy and palaeoecology of two Late Pleistocene species of vesicomyid bivalves from cold methane seeps at Svalbard (79°N). *Journal of Molluscan Studies*, **83**, 270–279.

Hoff, U., Rasmussen, T. L., Stein, R., Ezat, M. M. & Fahl, K. 2016. Sea ice and millenial-scale climate variability in the Nordic seas 90 kyr ago to present. *Nature communications*, **7**, 1–10.

Hryniewicz, K., Little, C. T. S. & Nakrem, H. A. 2014. Bivalves from the latest Jurassic–earliest Cretaceous hydrocarbon seep carbonates from central Spitsbergen, Svalbard. *Zootaxa*, **3859**, 1–66.

Hryniewicz, K., Hagström, J., Hammer, Ø., Kaim, A., Little, C. T. S. & Nakrem, H. A. 2015a. Late Jurassic-Early Cretaceous hydrocarbon seep boulders from Novaya Zemlya and their faunas. *Palaeogeography, Palaeoclimatology, Palaeoecology*, **436**, 231–244.

Hryniewicz, K., Nakrem, H. A., Hammer, Ø., Little, C. T. S., Kaim, A., Sandy, M. R. & **Hurum, J. H.** 2015b. The palaeoecology of the latest Jurassic-earliest Cretaceous hydrocarbon seep carbonates from Spitsbergen, Svalbard. *Lethaia*, **48**, 353–374.

Huber, M. 2010. *Compendium of bivalves. A full-color guide to 3,300 of the world's marine bivalves. A status on Bivalvia after 250 years of research*. ConchBooks, Hackenheim, 901 pp., 1 CD-ROM.

Huber, M. 2015. *Compendium of bivalves 2. A full-color guide to the remaining seven families. A systematic listing of 8'500 Bivalve species and 10'500 synonyms*. ConchBooks, Harxheim, 907 pp., 1 CD-ROM.

Jessen, S. P., Rasmussen, T. L., Nielsen, T. & **Solheim, A.** 2010. A new Late Weichselian and Holocene marine chronology for the western Svalbard slope 30,000–0 cal years BP. *Quaternary Science Reviews*, **29**, 1301–1312.

Kamenev, G. M. 2009. North Pacific species of the genus *Solemya* Lamarck, 1818 (Bivalvia: Solemyidae), with notes on *Acharax johnsoni* (Dall, 1891). *Malacologia*, **51**, 233–261.

Kamenev, G. M. 2017. Bivalve molluscs of the abyssal zone of the Sea of Okhotsk: Species composition, taxonomic remarks, and comparison with the abyssal fauna of the Pacific Ocean. *Deep-Sea Research Part II*. doi.org/10.1016/j.dsr2.2017.10.006

Kanehara, K. 1937. On some Tertiary fossil shells from Hokkaido (Yesso). *Japanese Journal of Geology and Geography*, **14**, 155–161.

Kanie, Y. & Kuramochi, T. 1995. *Acharax yokosukensis*, n. sp. (gigantic Bivalve) from the Miocene Hayama Formation of the Miura Peninsula, south-central Japan. *Science Report of Yokosuka City Museum*, **43**, 51–57.

Kanno, S. 1960. Palaeontology. *In* Arai, J. & Kanno, S.: *The Tertiary System of the Chichibu Basin, Saitama Prefecture, Central Japan*. Part II. Japan Society for the Promotion of Science, Ueno, Tokyo, 123–396.

Krylova, E. M., Gebruk, A. V., Portnova, D. A., Todt, C. & Haflidason, H. 2011. New species of the genus Isorropodon (Bivalvia: Vesicomyidae: Pliocardiinae) from cold methane seeps at Nyegga (Norwegian Sea, Vøring Plateau, Storrega Slide). *Journal of the Marine Biological Association of the United Kingdom*, **91**, 1135–1144.

Kuznetsov, A. P. & Shileyko, A. A. 1984. On the Gutless Protobranchia (Bivalvia). *Biologicheskie Nauki (Moscow)*, **2**, 39–49.

Levin, L. A., Baco, A. R., Bowden, D., Colaço, A., Cordes, E., Cunha, M. R., Demopoulos, A. W. J., Gobin, J., Grupe, B. M., Le, J., Metaxas, A., Netburn, A. N., Rouse, G. W., Thurber, A. R., Tunnicliffe, V., Dover, C. L. V., Vanreusel, A. & Watling, L. 2016. Hydrothermal vents and methane seeps: rethinking the sphere of influence. *Frontiers in Marine Science*, **3(72)**, 1–23.

Linnaeus, C. 1758. *Systema Naturae per regna tria naturae, secundum Classes, Ordines, Genera, Species*. Halae Magdeburgicae. 10th edition.

Mangerud, J., Bondevik, S., Gulliksen, S., Hufthammer, A. K. & Høisæter, S. 2006. Marine ^{14}C reservoir ages for 19th century whales and molluscs from the North Atlantic. *Quaternary Science Reviews*, **25**, 3228–3245.

Mau, S., Römer, M., Torres, M. E., Bussmann, I., Pape, T., Damm, E., Geprägs, P., Wintersteller, P., Hsu, C. W., Loher, M. & Bohrmann, G. 2017. Widespread methane seepage along the continental margin off Svalbard - from Bjørnøya to Kongsfjorden. *Scientific Reports*, **7(42997)**, 1–13.

Mayer, M. C. 1861. Description de Coquilles fossiles des terrains tertiaires supérieurs. *Journal de Conchyliologie, 3c série*, **9**, 358–373.

Métivier, B. & Cosel, R. von 1993. *Acharax alinae* n. sp., Solemyidae (Mollusca: Bivalvia) géante du bassin de Lau. *Comptes Rendus de l'Academie des Sciences Serie III Sciences de la Vie,* **316**, 229–237.

Mienert, J. 2013. *CAGE Cruise Report for 08 October 2013–25 October 2013 on Board the FF Helmer Hanssen*. 42 pp., The Arctic University of Tromsø, Tromsø, Norway.

Moore, E. J. 1963. Mollusks from the Astoria Formation in Oregon. *Geological Survey Professional Paper*, **419**, 1–109.

Natori, H. 1964. Some Molluscan Fossils from the Tertiary Muro Group in the Kii Peninsula, Japan. *Transactions and proceedings of the Palaeontological Society of Japan, New Series*, **55**, 247–255, pl. 36.

Neulinger, S. C., Sahling, H., Süling, J. & Imhoff, J. F. 2006. Presence of two phylogenetically distinct groups in the deep-sea mussel *Acharax* (Mollusca: Bivalvia: Solemyidae). *Marine Ecology Progress Series*, **312**, 161–168.

Oliver, P. G., Rodrigues, C. F. & Cunha, M. R. 2011. Chemosymbiotic bivalves from the mud volcanoes of the Gulf of Cadiz, NE Atlantic, with descriptions of new species of Solemyidae, Lucinidae and Vesicomyidae. *ZooKeys*, **113**, 1–38.

Olsson, A. A. 1931. Contributions to the Tertiary Paleontology of Northern Peru; Part 4, The Peruvian Oligocene. *Bulletins of American Paleontology*, **17(63)**, 97–264.

Olsson, A. A. 1942. Tertiary and Quaternary fossils from the Burica Peninsula of Panama and Costa Rica. *Bulletin of American Paleontology*, **27(106)**, 1–96.

Patton, H., Andreasen, K., Bjarnadóttir, L. R., Dowdeswell, J. A., Winsborrow, M. C. M., Noormets, R., Polyak, L., Auriac, A. & Hubbard, A. 2015. Geophysical constraints on the dynamics and retreat of the Barents Sea ice sheet as a paleobenchmark for models of marine ice sheet deglaciation. *Reviews of Geophysics*, **53**, 1051–1098.

Paull, C. K., Dallimore, S. R., Caress, D. W., Gwiazda, R., Melling, H., Riedel, M., Jin, Y. K., Hong, J. K., Kim, Y.-G., Graves, D., Sherman, A., Lundsten, E., Anderson, K., Lundsten, L., Villinger, H., Kopf, A., Johnson, S. B., Clarke, J. H., Blasco, S., Conway, K., Neelands, P., Thomas, H. & Côté, M. 2015. Active mud volcanoes on the

continental slope of the Canadian Beaufort Sea. *Geochemistry, Geophys Geosystems*, **16,** 3160–3181

Pedersen, R. B.; Rapp, H. T., Thorseth, I. H., Lilley, M. D., Barriga, F. J. A. S., Baumberger, T., Flesland, K., Fonseca, R., Früh-Green, G. L. & Jorgensen, S. L. 2010. Discovery of a black smoker vent field and vent fauna at the Arctic Mid-Ocean Ridge. *Nature Communication*, **1(126)**, 1–6.

Plaza-Faverola, A., Bünz, S., Johnson, J. E., Chand, S., Knies, J., Mienert, J. & Franek, P. 2015. Role of tectonic stress in seepage evolution along the gas hydrate-charged Vestnesa Ridge, Fram Strait. *Geophysical Research Letters*, **42**, 733–742.

Portnov, A., Vadakkepuliyambatta, S., Mienert, J. & **Hubbard, A.** 2016. Ice-sheet-driven methane storage and release in the Arctic. *Nature Communication*, **7(10314)**, 1–7.

Rachor, E. (ed.) 1997. Scientific cruise report of the Arctic expedition ARK-XI/1 of RV "Polarstern" in 1995. German-Russian project LADI: Laptev Sea – Arctic deep basin interrelations. *Berichte zur Polarforschung*, **226**, 157 pp + appendix.

Rasmussen, T. L. & **Thomsen, E.** 2004. The role of the North Atlantic Drift in the millennial timescale glacial climate fluctuations. *Palaeogeography, Palaeoclimatology, Palaeoecology*, **210**, 101–116.

Rasmussen, T. L., Thomsen, E., Ślubowska, M. A., Jessen, S., Solheim, A. & **Koç, N.** 2007. Paleoceanographic evolution of the SW Svalbard margin (76°N) since 20,000 ^{14}C yr BP. *Quaternary Research*, **67**, 100–114.

Rasmussen, T. L., Thomsen, E., & **Nielsen, T**. 2014. Water mass exchange between the Nordic seas and the Arctic Ocean on millennial time scale during MIS 4–MIS 2. *Geochemistry, Geophysics, Geosystems*, **15**, 530–544.

Rasmussen, T. L., Nielsen, T., Kuijpers, A., Sztybor, K., Ezat, M., Jessen, S. P. & **Dijkstra, N.** 2015. *Cruise Report, GEO8144/3144 – Greenhouse Gases in the Ocean:*

Marine Geology and Geophysics Cruise on R/V Helmer Hanssen, July 23rd – August 3rd 2015. Department of Geology, UiT, Arctic University of Norway, NO-9037 Tromsø, Norway. 1–26.

Rasmussen, T.L., Nielsen, T., Ofstad, S., Åström, E., Altuna, N. E. B., Laier, T., Sen, A., Chitkara, C., Frolova, A. & Mamadzhanian, A. 2018. CAGE-18-3 Cruise to the Barents Sea, Storfjorden Trough, East Greenland Ridge (Leg 1, 2), Arctic Ocean, Vestnesa Ridge, and PKF (Leg 3). Department of Geosciences, Uit, the Arctic University of Norway, pp. 1–36.

Reimer, P. J., Bard, E., Bayliss, A., Beck, J. W., Blackwell, P. G., Ramsey, C. B., Buck, C. E., Cheng, H., Edwards, R. L., Friedrich, M., Grootes, P. M., Guilderson, T. P., Haflidason, H., Hajdas, I., Hatté, C., Heaton, T. J., Hoffmann, D. L., Hogg, A. G., Hughen, K. A., Kaiser, K. F., Kromer, B., Manning, S. W., Niu, M., Reimer, R. W., Richards, D. A., Scott, E. M., Southon, J. R., Staff, R. A., Turney, C. S. M. & Plicht, J. v. d. 2013. IntCal13 and Marine13 Radiocarbon Age Calibration Curves 0–50,000 Years cal BP. *Radiocarbon*, **55**, 1869–1887.

Rueda, J. L., Urra, J., Gofas, S., López-González, N., Fernández-Salas, L. M. & Díaz-Del-Río, V. 2012. New records of recently described chemosymbiotic bivalves for mud volcanoes within the European waters (Gulf of Cádiz). *Mediterranean Marine Science*, **13**, 262–267.

Schander C, Rapp H.T, Kongsrud J.A, Bakken T, Berge J, Cochrane S, Oug E, Byrkjedal I, Todt C, Cedhagen T, Fosshagen A, Gebruk A, Larsen K, Levin L.A, Obst M, Pleijel F, Stöhr S, Warén A, Mikkelsen N.T, Hadler-Jacobsen S, Keuning R, Petersen K.H, Thorseth I.H & Pedersen R.B, 2010 The fauna of hydrothermal vents on the Mohn Ridge (North Atlantic). *Marine Biology Research*, **6,** 155–171.

Sahling, H., Galkin, S. V., Salyuk, A., Greinert, J., Foerstel, H., Piepenburg, D. & Suess,

E. 2003. Depth-related structure and ecological significance of cold-seep communities—a case study from the Sea of Okhotsk. *Deep Sea Research Part I Oceanographic Research Papers*, **50**, 1391–1409.

Sahling, H., Römer, M., Pape, T., Bergès, B., Fereirra, C. d. S., Boelmann, J., Geprägs, P., Tomczyk, M., Nowald, N., Dimmler, W., Schroedter, L., Glockzin, M. & **Bohrmann, G.** 2014. Gas emissions at the continental margin west of Svalbard: mapping, sampling, and quantification. *Biogeosciences*, **11**, 6029–6046.

Sasaki, T., Okutani, T. & **Fujikura K.** 2005. Molluscs from hydrothermal vents and cold seeps in Japan: a review of taxa recorded in twenty Recent years (1984–2004). *Venus*, **64**, 87–133.

Savvichev, A. S., Kadnikov, V. V., Kravchishina, M. D., Galkin, S. V., Novigatskii, A. N., Sigalevich, P. A., Merkel, A. Y., Ravin, N. V., Pimenov, N. V. & **Flintet, M. V.** 2018. Methane as an organic matter source and the trophic basis of a Laptev Sea cold seep microbial community. *Geomicrobiology Journal*, **35**, 411–423.

Sen, A., Åström, E. K. L., Hong, W.-L., Portnov, A., Waage, M., Serov, P., Carroll, M. L. & **Carroll, J.** 2018. Geophysical and geochemical controls on the megafaunal community of a high Arctic cold seep. *Biogeosciences*, **15**, 4533–4559.

Smith, E. A. 1885. Report on the Lamellibranchiata collected by H.M.S. Challenger during the years 1873 – 1876. In: Report on the scientific results of the voyage of H.M.S. Challenger during the years 1873 – 1876. *Zoology, London*, **13(35)**, 1–341.

Stuiver, M. & **Reimer, P. J.** 1993. Extended ^{14}C data base and revised CALIB 3.0 14C age calibration program. *Radiocarbon*, **35**, 215–230.

Sweetman, A. K., Levin, L. A., Rapp, H. T. & Schander, C. 2013. Faunal trophic structure at hydrothermal vents on the southern Mohn's Ridge, Arctic Ocean. *Marine Ecology Progress Series*, **473**, 115–131.

Sztybor, K. & **Rasmussen, T. L.** 2017a. Diagenetic disturbances of marine sedimentary records from methane-influenced environments in the Fram Strait as indications of variation in seep intensity during the last 35 000 years. *Boreas*, **46**, 212–228.

Sztybor, K. & **Rasmussen, T. L.** 2017b. Late glacial and deglacial palaeoceanographic changes at Vestnesa Ridge, Fram Strait: Methane seep versus non-seep environments. *Palaeogeography, Palaeoclimatology, Palaeoecology*, **476**, 77–89.

Taviani, M., Angeletti, L. & Ceregato, A. 2011. Chemosynthetic bivalves of the family Solemyidae (Bivalvia, Protobranchia) in the Neogene of the Mediterranean Basin. *Journal of Paleontology*, **85**, 1067–1076.

Taylor, J. D. & **Glover, E. A.** 2010. Chapter 5, Chemosymbiotic Bivalves. in: S. Kiel (ed.), The Vent and Seep Biota. *Topics in Geobiology*, **33**, 107–135.

Tomczak, M. & Godfrey, J. S. 1994. *Regional Oceanography: An Introduction*. Pergamon Press, Oxford, 422 pp, 1. edition.

Uchida, M., Ohkushi, K., Kimoto, K., Inagaki, F., Ishimura, T., Tsunogai, U., TuZino, T. & **Shibata, Y.** 2008. Radiocarbon-based carbon source quantification of anomalous isotopic foraminifera in last glacial sediments in the western North Pacific. *Geochemistry, Geophysics, Geosystems*, **9**, Q04N14, 1–26.

Vanreusel, A., Andersen, A. C., Boetius, A., Cunha, M. R., Decker, C., Hilario, A., Kormas, K. A., Maignien, L., Olu, K., Pachiadaki, M., Ritt, B., Rodrigues, C., Sarrazin, J., Tyler, P., Gaever, S. Van & Vanneste, H. 2009. Biodiversity of Cold Seep Ecosystems Along the European Margins. *Oceanography*, **22**, 110–127.

Verrill, A. E. & **Bush, K. J.** 1898. Revision of the deep-water Mollusca of the Atlantic coast of North America, with descriptions of new genera and species. *Proceedings of the United States National Museum*, **20**, 775–901.

Vokes, H. E. 1955. Notes on Tertiary and Resent Solemyacidae. *Journal of Paleontology*, **29**, 534–545.

Vokes, H. E. 1970. Two new species of deep water bivalves from the Caribbean Sea. *Veliger*, **12**, 357–361.

Walton, K. 2015. New Zealand living Solemyidae (Bivalvia: Protobranchia). *Molluscan Research*, **35**, 246–261.

Westbrook, G. K., Thatcher, K. E., Rohling, E. J., Piotrowski, A. M., Pälike, H., Osborne A. H., Nisbet, E. G., Minshull, T. A., Lanoisellé, M., James, R. H., Hühnerbach, V., Green, D., Fisher, R. E., Crocker, A. J., Chabert, A., Bolton, C., Beszczynska-Möller, A., Berndt, C. & Aquilina, A. 2009. Escape of methane gas from the seabed along the West Spitsbergen continental margin. *Geophysical Research Letters*, **36(15)**, 1–5.

Zachos, J., Pagani, M., Sloan, L., Thomas, E. & Billups, K. 2001. Trends, rhythms, and aberrations in global climate 65 Ma to present. *Science*, **292**, 686–693.

Zakharov, V., Shurygin, B. N., Kurushin, N. I., Meledina, S. V. & Nikitenko, B. L. 2002. A Mesozoic ocean in the Arctic: Paleontological evidence. *Russian Geology and Geophysics*, **43**, 143–170.

Table 1. Conventional AMS-^{14}C dates and calibrated ages for core HH15-1241GC.

Table 2. Comparative table of Neogene *Acharax* species. *Original description and/or present information based on one specimen. Valve length is for calcified part.

Figure 1. Map showing location of Vestnesa Ridge. A: Overview map of the Nordic seas indicating main surface currents. B: Map of Svalbard archipelago with red squares marking known methane seep areas of Vestnesa Ridge, off Prins Karls Forland and Storfjord Trough. Black circles mark eleven core sites from Svalbard western margin used in creating a stack record of stratigraphy for the western Svalbard margin shown in Figure 2 (see text for explanation and Jessen *et al.* (2010)). C: Enlargement of Vestnesa seepage area showing location of the cores from which *Acharax svalbardensis* n. sp. was collected; red star marks location of type core HH15-1241GC; red circles mark other cores with *Acharax svalbardensis* and vesicomyid bivalves (this study; Ambrose *et al.* 2015; Sztybor & Rasmussen 2017a, b). A and B modified from Jessen *et al.* (2010); C modified from Sztybor & Rasmussen (2017a) based on data from Bünz *et al.* (2012).

Figure 2. Stratigraphy, calibrated ^{14}C ages and correlation of studied cores with previously published records. The stack record is modified from Jessen *et al.* (2010). Ages in italics are transferred ages from other cores (see Jessen *et al.* 2010). Core JM10-335GC is modified from Sztybor & Rasmussen (2017a) and cores HH13-211GC and -203GC are modified from Ambrose *et al.* (2015). Column to the left shows known event stratigraphy of the western Svalbard margin (e.g., Rasmussen *et al.* 2007; Jessen *et al.* 2010). Abbreviations: H, Holocene interglacial; YD, Younger Dryas stadial; A, Allerød interstadial; B, Bølling interstadial; H1, Heinrich event H1; LGM, Last Glacial Maximum. All ages are calibrated ^{14}C

ages (re-calibration of all new and published ages using Calib7.04 and Marine13 programs; see text for explanation). Ages marked with asterisks are considered as too old due to contamination by authigenic carbonates.

Figure 3. Drawings of the reconstructed holotype of *Acharax svalbardensis* n. sp. **A**, Left valve exterior; **B**, Left valve interior; **C**, Right valve exterior; **D**, Right valve interior. Abbreviations: aa, anterior adductor scar; apr, anterior pedal retractor scar; lig, ligament; ny, nymph; pa, posterior adductor scar; pl, pallial line. Dashed line in C and D marks outline of broken off valve margin.

Figure 4. *Acharax svalbardensis* n. sp. **A–F**. Holotype (TSGF 18407). **A**, Exterior of left valve; **B**, Interior of left valve; **C**, Dorsal view of left valve; **D**, Dorsal view of umbonal part of right valve; **E**, Exterior of right valve; **F**, Interior of right valve. Core HH15-1241GC, Vestnesa Ridge, Fram Strait, NW Spitsbergen, Svalbard archipelago, 79°00.214´N, 06°55.904´E, water depth 1205 m.

Figure 5. *Acharax svalbardensis* n. sp. **A, B.** TSGF 18408, RV fragment. **A,** Exterior; **B,** Interior. **C, D.** TSGF 18409, RV fragment. **C,** Exterior; **D,** Interior. **E–G.** TSGF 18410, LV. **E,** Exterior; **F,** Interior; **G**, dorsal view. **H–I.** RV of same specimen. **H,** Exterior; **I,** Interior. **J, K.** TSGF 18411, LV. **J,** Exterior; **K,** Interior. **L, M.** TSGF 18412, LV. **L,** Exterior; **M,** Interior. **N–O.** TSGF 18413, LV fragment. **N,** Exterior; **O,** Interior. **P, Q.** TSGF 18414, LV fragment. **P**, Exterior; **Q,** Interior. **R, S.** TSGF 18415, RV. **R,** Exterior; **S,** Interior. **T, U.** TSGF 18416, RV. **T,** Exterior; **U,** Interior. **V, W.** TSGF 18417, LV. **V,** Exterior; **W,** Interior.

Table 1.

Depth (cm)	Material	Laboratory Code	Age (^{14}C a yr BP)	Age (cal. yr BP)
199.5	*N. pachyderma*	UBA-36332	17,270 ± 82	20,347 ± 127
244.5	*N. pachyderma*	UBA-36333	17,385 ± 77	20,481 ± 115
329.5	*N. pachyderma*	UBA-36344	23,231 ± 136	27,205 ± 155
494.0	*N. pachyderma*	UBA-36345	27,341 ± 238	31,020 ± 144

Table 2

	Period	L (mm)	H/L	Umbo from posterior margin (%L)	Ribs	Strength of middle ribs	Anterodorsal corner
Acharax svalbardensis n. sp.	Pleistocene	~70	~0.35 (0.32–0.35)	27–30	15	about as posterior	rounded to perpendicular
Acharax alinae Métivier & Cosel, 1993	Recent	106	0.43	~33	16–17	about as posterior	generally pointed
Acharax bartschii (Dall, 1908b)*	Recent	191*	0.32*	36*	14–15*	absent*	pointed*
Acharax burica Olsson, 1942*	Pliocene	~115*	0.41*	~33*	20–21*	about as posterior*	?
Acharax caribbaea (Vokes, 1970)*	Recent	78	0.36–0.41	~27	14–15	poorly developed	perpendicular to slightly pointed
Acharax clarificata Dell, 1995	Recent	88	0.36–0.39	~28–30	~16	poorly developed	rounded to perpendicular
Acharax doderleini (Mayer, 1861)*	Miocene-Pliocene	101	~0.30 (0.28–0.33)	23–27	?	poorly developed	generally pointed
Acharax gadirae Oliver, Rodrigues & Cunha, 2011	Recent	67	~0.37 (0.37–0.48)	25–32	15–16	poorly developed	generally pointed
Acharax gigas (Kanno, 1960)	Miocene	264	0.25–0.35	22–35	?	poorly developed	rounded
Acharax grandis (Verrill & Bush, 1898)	Recent	≥70	~0.36	28	16–19	weaker developed	rounded to perpendicular
Acharax johnsoni (Dall, 1891)* species complex	Miocene-Recent	150 (holotype 115)	0.42 (holotype)	23–30	14–15	generally weaker	variable
Acharax muroensis (Natori, 1964)*	Oligocene-Miocene	>22*	?	~20*	?	strongest*	pointed*
Acharax patagonica (Smith, 1885)*	Recent	62	~32–35	~25–28	~17–18	absent or weaker developed	rounded
Acharax prashadi (Vokes, 1955)	Recent	100	0.33–0.36	22–27	9–?	absent or poorly developed	slightly pointed
Acharax subquadrata (Foresti, 1879)*	Miocene	86	0.38–0.41	~24	?	about as posterior	angular, slightly pointed to perpendicular
Acharax subventricosta Krishtofovich in Gladenkov *et al.* (1984)*	Neogene	~50*	~0.4*	~33*	?	?	rounded to perpendicular*
Acharax ventricosa (Conrad, 1849)	Miocene-Pliocene	>100	~0.35–0.44	~29–36	?	poorly developed	generally pointed
Acharax yessoensis (Kanehara, 1937)*	Miocene	84*	0.31*	~29*	?	poorly developed*	pointed*
Acharax yokosukensis Kanie & Kuramochi, 1995	Miocene	>296	0.39–0.44	39–48	11–14	finer and weaker	rounded to pointed

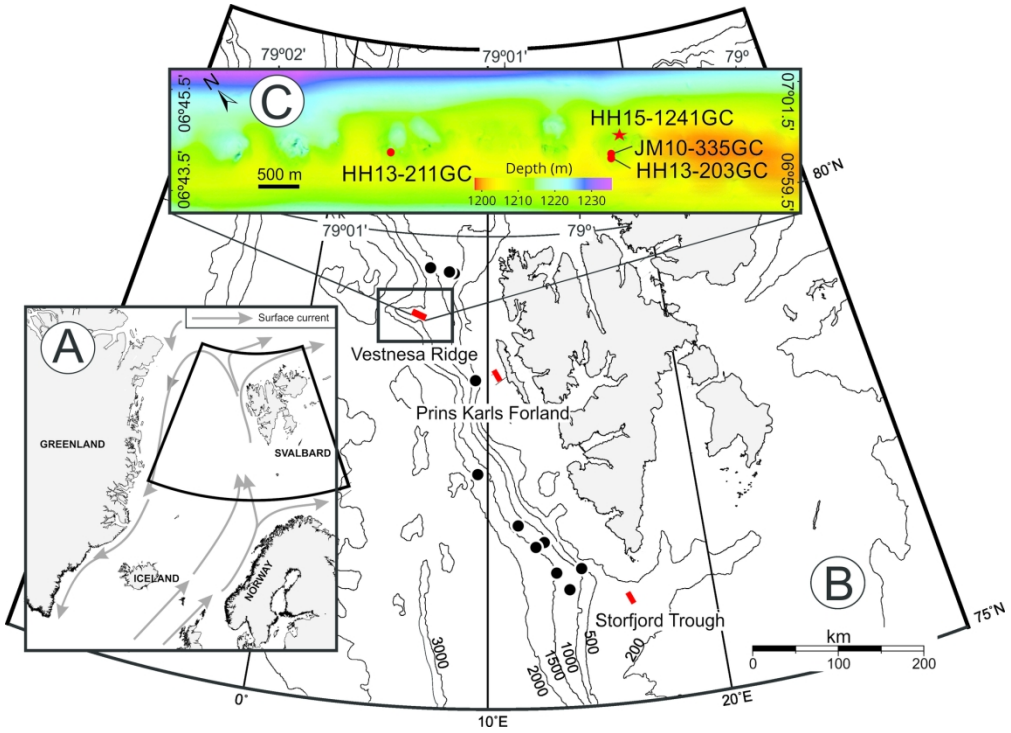

Figure 1. Map showing location of Vestnesa Ridge. A: Overview map of the Nordic seas indicating main surface currents. B: Map of Svalbard archipelago with red squares marking known methane seep areas of Vestnesa Ridge, off Prins Karls Forland and Storfjord Trough. Black circles mark eleven core sites from Svalbard western margin used in creating a stack record of stratigraphy for the western Svalbard margin shown in Figure 2 (see text for explanation and Jessen et al. (2010)). C: Enlargement of Vestnesa seepage area showing location of the cores from which Acharax svalbardensis n. sp. was collected; red star marks location of type core HH15-1241GC; red circles mark other cores with Acharax svalbardensis and vesicomyid bivalves (this study; Ambrose et al. 2015; Sztybor & Rasmussen 2017a, b). A and B modified from Jessen et al. (2010); C modified from Sztybor & Rasmussen (2017a) based on data from Bünz et al. (2012).

172x125mm (300 x 300 DPI)

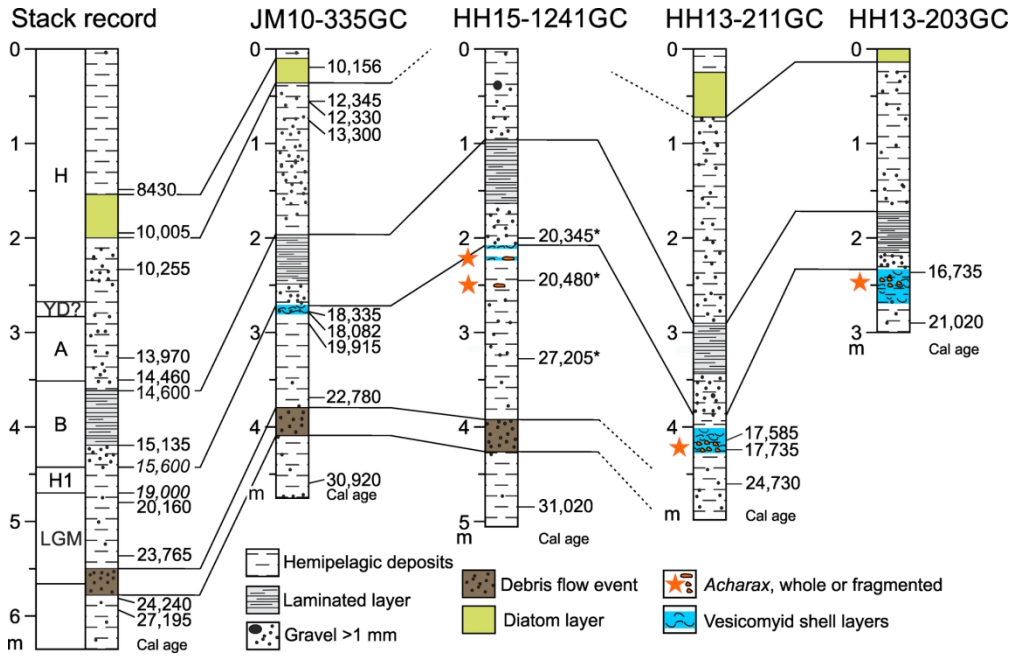

Figure 2. Stratigraphy, calibrated 14C ages and correlation of studied cores with previously published records. The stack record is modified from Jessen et al. (2010). Ages in italics are transferred ages from other cores (see Jessen et al. 2010). Core JM10-335GC is modified from Sztybor & Rasmussen (2017a) and cores HH13-211GC and -203GC are modified from Ambrose et al. (2015). Column to the left shows known event stratigraphy of the western Svalbard margin (e.g., Rasmussen et al. 2007; Jessen et al. 2010). Abbreviations: H, Holocene interglacial; YD, Younger Dryas stadial; A, Allerød interstadial; B, Bølling interstadial; H1, Heinrich event H1; LGM, Last Glacial Maximum. All ages are calibrated 14C ages (re-calibration of all new and published ages using Calib7.04 and Marine13 programs; see text for explanation). Ages marked with asterisks are considered as too old due to contamination by authigenic carbonates.

172x111mm (300 x 300 DPI)

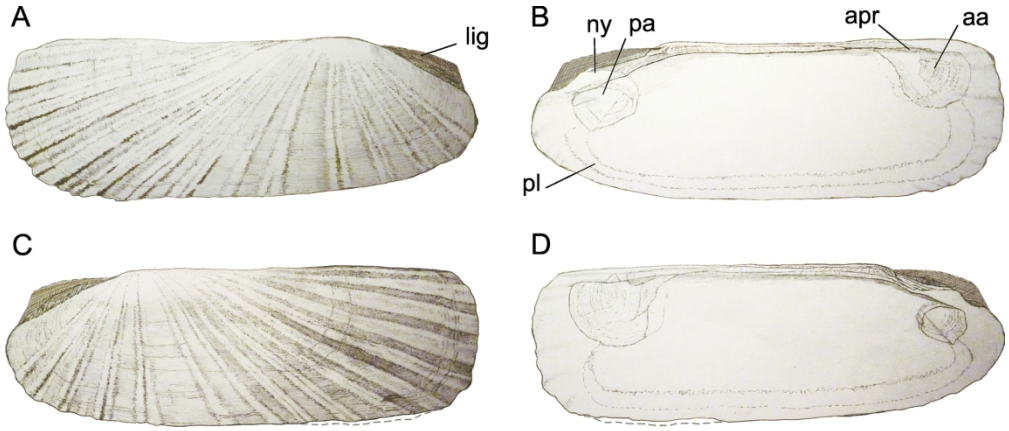

Figure 3. Drawings of the reconstructed holotype of Acharax svalbardensis n. sp. A, Left valve exterior; B, Left valve interior; C, Right valve exterior; D, Right valve interior. Abbreviations: aa, anterior adductor scar; apr, anterior pedal retractor scar; lig, ligament; ny, nymph; pa, posterior adductor scar; pl, pallial line. Dashed line in C and D marks outline of broken off valve margin.

173x72mm (300 x 300 DPI)

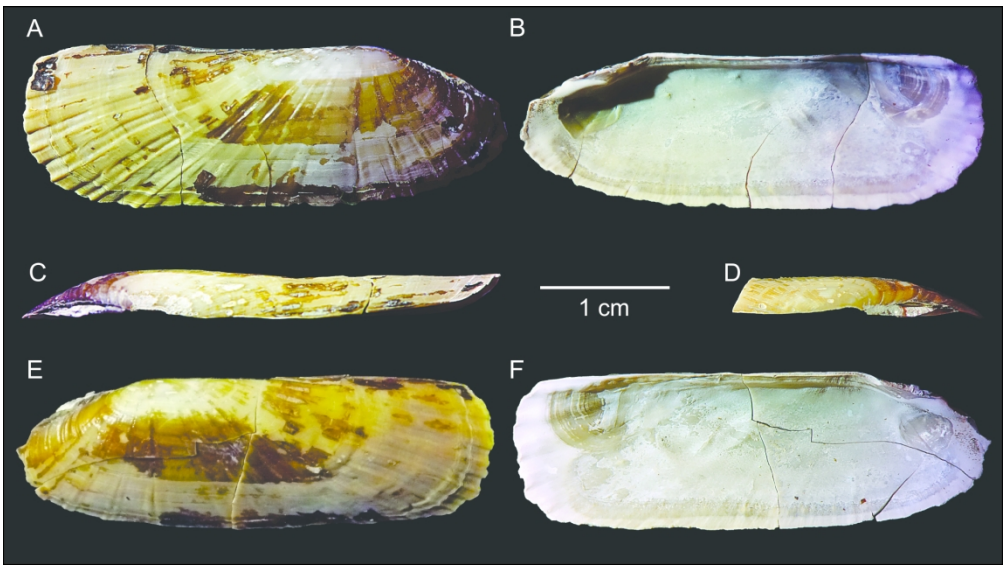

Figure 4. Acharax svalbardensis n. sp. A–F. Holotype (TSGF ----1). A, Exterior of left valve; B, Interior of left valve; C, Dorsal view of left valve; D, Dorsal view of umbonal part of right valve; E, Exterior of right valve; F, Interior of right valve. Core HH15-1241GC, Vestnesa Ridge, Fram Strait, NW Spitsbergen, Svalbard archipelago, 79°00.214′N, 06°55.904′E, water depth 1205 m.

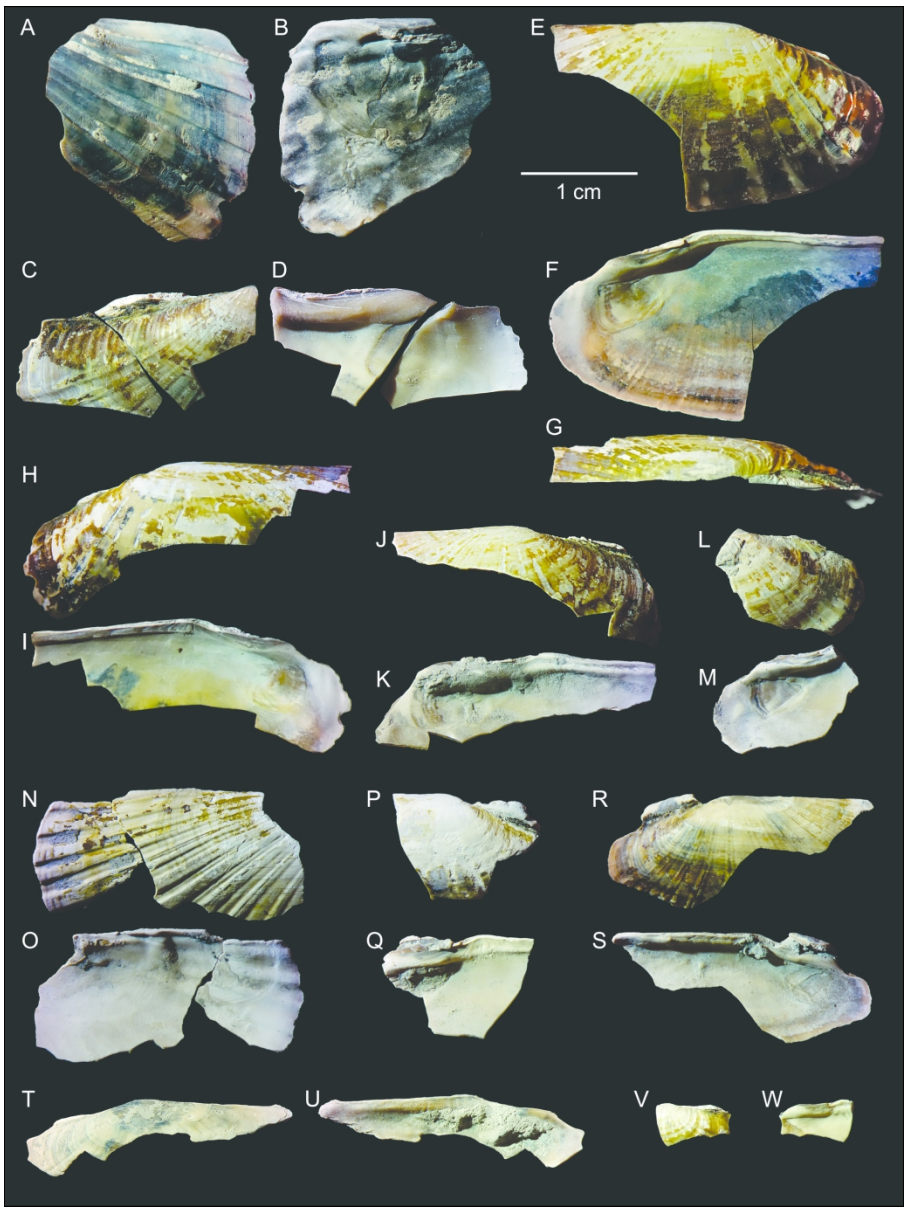

Figure 5. Acharax svalbardensis n. sp. a, b. TSGF ----2, RV fragment. a. Exterior. b. Interior. c, d. TSGF ----3, RV fragment. c. Exterior. d. Interior. e–g. TSGF ----4, LV. e. Exterior. f. Interior. g. dorsal view. h–i. TSGF ----5, RV. h. Exterior. i. Interior. j, k. TSGF ----6, LV. j. Exterior. k. Interior. l, m. TSGF ----7, LV. l. Exterior. m. Interior. n–o. TSGF ----8, LV fragment. n. Exterior. o. Interior. p, q. TSGF ----9, LV fragment. p. Exterior. q. Interior. r, s. TSGF ----10, RV. r. Exterior. s. Interior. t, u. TSGF ----11, RV. t. Exterior. u. Interior. v, w. TSGF ----12, LV. v. Exterior. w. Interior.

173x230mm (300 x 300 DPI)